Published in final edited form as:
Dev Cell. 2014 November 10; 31(3): 291–304. doi:10.1016/j.devcel.2014.09.012.

The conserved Misshapen-Warts-Yorkie pathway acts in enteroblasts to regulate intestinal stem cells in *Drosophila*

Qi Li[1], **Shuangxi Li**[4], **Sebastian Mana-Capelli**[2], **Rachel J. Roth Flach**[1], **Laura V. Danai**[1], **Alla Amcheslavsky**[1], **Yingchao Nie**[1], **Satoshi Kaneko**[1], **Xiaohao Yao**[1], **Xiaochu Chen**[1], **Jennifer L. Cotton**[3], **Junhao Mao**[3], **Dannel McCollum**[2], **Jin Jiang**[4], **Michael P. Czech**[1], **Lan Xu**[1,#,*], and **Y. Tony Ip**[1,*]

[1]Program in Molecular Medicine, University of Massachusetts Medical School, Worcester, MA 01605, USA

[2]Department of Biochemistry and Molecular Pharmacology, University of Massachusetts Medical School, Worcester, MA 01605, USA

[3]Department of Cancer Biology, University of Massachusetts Medical School, Worcester, MA 01605, USA

[4]Department of Developmental Biology, University of Texas Southwestern Medical Center, Dallas, TX 75390, USA

SUMMARY

Similar to the mammalian intestine, the *Drosophila* adult midgut has resident stem cells that support growth and regeneration. How the niche regulates intestinal stem cell activity in both mammals and flies is not well understood. Here we show that the conserved germinal center protein kinase Misshapen restricts intestinal stem cell division by repressing the expression of the JAK-STAT pathway ligand Upd3 in differentiating enteroblasts. Misshapen, a distant relative to the prototypic Warts activating kinase Hippo, interacts with and activates Warts to negatively regulate the activity of Yorkie and the expression of Upd3. The mammalian Misshapen homolog MAP4K4 similarly interacts with LATS (Warts homolog) and promotes inhibition of YAP (Yorkie homolog). Together, this work reveals that the Misshapen-Warts-Yorkie pathway acts in enteroblasts to control niche signaling to intestinal stem cells. These findings also provide a model

Correspondence: Tony Ip, Tony.Ip@umassmed.edu. Lan Xu, LXu@blueprintmedicines.com.
[#]Present address: Blueprint Medicines, 215 First street, Cambridge, MA 02142, USA
[*]equal contribution

Author Contributions

QL, LX and YTI conceived the project. QL, AA, YN carried out the Drosophila molecular genetic analyses. XY, SK, XC, LX, AA, JLC and JM performed Msn biochemical analyses in S2 cells, generation of mutant Msn transgenic flies and expression analysis of MAP4K4 and related kinases in mouse intestine. SM-C and DM carried out the experiments for mammalian LATS and YAP. SL and JJ performed the experiments for the Drosophila Wts and Yki in S2 cells. RJRF, LVD and MPC carried out the MAP4K4 knockout mouse and MEF isolation. QL, LX and YTI wrote the manuscript and all authors amended the manuscript.

in which to study requirements for MAP4K4-related kinases in MST1/2-independent regulation of LATS and YAP.

Keywords

Drosophila; enteroblasts; intestine; Misshapen; MAP4K4; stem cells; Warts; Yorkie

INTRODUCTION

Similar to most other adult organs, the GI tract contains resident stem cells that support tissue homeostasis (Grompe, 2012). In the mammalian intestine, two groups of stem cells called label retention cells (LRCs) and columnar base cells (CBCs) located near the base of each crypt together function to replenish lost cells along the crypt-villus axis (Barker et al., 2007; Sangiorgi and Capecchi, 2008; Takeda et al., 2011; Tan and Barker, 2014; Tian et al., 2011; Yan et al., 2012; Zhu et al., 2009). Intestinal stem cells (ISCs) are thought to be regulated by surrounding niche cells, however the detailed mechanisms underlying this regulation remain poorly understood (Tan and Barker, 2014).

In the *Drosophila* adult midgut, ISCs are evenly distributed along the basal side of the epithelium (Micchelli and Perrimon, 2006; Ohlstein and Spradling, 2006). ISCs are the only mitotic cells in the adult midgut and therefore are critical for intestinal homeostasis. After an ISC division, Delta-Notch signaling establishes the asymmetry between the renewed ISC and the neighboring enteroblast (EB) (Ohlstein and Spradling, 2007; Perdigoto et al., 2011). Although the mechanism that establishes the asymmetric Delta is largely unknown, it is clear that the strength of Notch pathway stimulation is a key to determinant of whether the EB differentiates to become an enterocyte (EC) for nutrient absorption or an enteroendocrine cell (EE) for hormone secretion (Fig. 1K) (de Navascues et al., 2012; Goulas et al., 2012; Kapuria et al., 2012; Ohlstein and Spradling, 2007; Perdigoto et al., 2011).

Many conserved signaling pathways regulate *Drosophila* ISC division. EGF and JAK-STAT pathways regulate ISC division and subsequent differentiation and therefore are essential for midgut homeostasis (Beebe et al., 2010; Biteau and Jasper, 2011; Buchon et al., 2010; Jiang et al., 2010; Liu et al., 2010; Ragab et al., 2011; Xu et al., 2011; Zhou et al., 2013). The Insulin receptor, TSC-TOR and Myc pathways are important for the coordination of midgut growth (Amcheslavsky et al., 2011; Amcheslavsky et al., 2009; Choi et al., 2011; Kapuria et al., 2012; Ren et al., 2013). The Hippo-Warts-Yorkie (Hpo-Wts-Yki) pathway has functions in both ECs and ISCs to regulate ISC division and regeneration (Huang et al., 2014; Karpowicz et al., 2010; Ren et al., 2010; Shaw et al., 2010; Staley and Irvine, 2010). Recent evidence suggests that ISC division and asymmetry are flexible and can adapt to environmental factors such as nutrient availability (O'Brien et al., 2011). Other evolutionarily conserved pathways such as Wingless, JNK, BMP and PVFs are also involved in the maintenance and stress response of ISCs (Bond and Foley, 2012; Choi et al., 2008; Guo et al., 2013; Hochmuth et al., 2011; Li et al., 2013a; Li et al., 2013b; Lin et al.,

2008; Tian and Jiang, 2014). How these many conserved regulatory pathways are coordinated to achieve intestinal homeostasis remains to be answered.

Here we show a niche mechanism that depends on Misshapen (Msn), a member of the germinal center protein kinase (GCK) family, acting within EBs to repress the expression of the JAK-STAT pathway ligand Upd3. Mechanistically, Msn function is independent of JNK or Hpo but instead interacts with Wts to suppress Yki activity and Upd3 expression. We also show that the mammalian Msn homolog MAP4K4 interacts with LATS to suppress YAP activity in mammalian cells, suggesting that this is an evolutionarily conserved mechanism possibly employed in various biological contexts.

RESULTS

Loss of Msn function in the adult midgut causes hyperplasia

To identify regulators essential for midgut homeostasis, we used the *escargot* promoter-Gal4; tubulin-Gal80^{ts}; UAS-mCD8GFP (esg^{ts}>GFP) as driver and marker to perform RNA interference (RNAi) assays of various genes. This driver is expressed in both ISCs and EBs (Fig. 1K), and the Gal80^{ts} temperature sensitive repressor provides temporal control of the Gal4 activity (Amcheslavsky et al., 2011; Micchelli and Perrimon, 2006). Two independent transgenic UAS-dsRNA lines (*msn*^{TRiP} and *msn*^{VDRC}) targeting non-overlapping sequences of *msn* caused a large increase of the number of GFP^{+} cells. Optical cross-sections indicated an intestinal hyperplasia phenotype (Fig. 1A–D). Knockdown of *msn* increased substantially the number of p-H3^{+} cells (Fig. 1E), a marker for mitotic ISCs (Micchelli and Perrimon, 2006; Ohlstein and Spradling, 2006). In all these experiments, *msn*^{RNAi} was induced by temperature shift in adult flies, so the hyperplasia phenotype is not a developmental defect.

To confirm that the dsRNA-induced phenotype was due to loss of Msn function, we performed a rescue experiment. Two independent transgenic lines carrying a full-length *msn* cDNA together with the RNAi construct showed an almost complete suppression of the midgut phenotype (Fig. 1F, *msn*$^{cDNA\text{-}1}$ and *msn*$^{cDNA\text{-}2}$). We further generated a construct that expressed the Msn^{768}, which retains the N-terminal 768 amino acids including the kinase domain and the middle segment but not the C-terminal region targeted by both dsRNA. Two independent transgenic lines containing this RNAi-insensitive construct (*msn*$^{768\text{-}1}$ and *msn*$^{768\text{-}2}$) also provided complete rescue of the ISC division phenotype induced by *msn*^{TRiP} (Fig. 1F).

Staining and quantification of various cell fate markers in the midgut suggest that an increased ISC proliferation, but not production of more ISCs through increased symmetric division, is the reason behind the hyperplasia phenotype. First, staining of *msn*^{RNAi} guts with the ISC-specific marker Delta showed a similar number and distribution of Delta+ cells compared to wild-type (Fig. 1G–H′, arrows). In contrast, *msn*^{RNAi} guts displayed a significant increase in the number of the daughter cell marker Su(H)lacZ, as well as esg>GFP (Fig. 1L–M′ and Supp Fig. S1A–D). Second, in *msn*^{RNAi} guts, almost all the p-H3^{+} cells also had Delta staining (control 100%, n=25; *msn*^{RNAi} 98%, n=48), and they were all basally located similar to the ISCs in wild type guts (Fig. 1I–J″). It is noteworthy that less than 1% of p-H3^{+} also contained Pros staining (Zielke et al., 2014), but the proportion of

this population did not change after msn^{RNAi} (Fig. S1E) and therefore should not contribute significantly to the over-proliferation phenotype. Third, quantification of mutant clones with multiple $Delta^+$ cells, which may come from fusion or symmetric division, revealed no change in the ratio over clones with single $Delta^+$ cells (Supp Fig. S2A), further suggest that *msn* mutants have similar ratio of ISC asymmetric/symmetric division as previously reported (Goulas et al., 2012; O'Brien et al., 2011). Therefore, various approaches demonstrate that loss of Msn causes increased ISC proliferation to generate more progeny cells and causes hyperplasia in the adult midgut.

Msn acts in EBs to regulate ISC division non-autonomously

Mutant clonal analysis was performed to validate the phenotype and gain insight into the cell type requirement of *msn* function. We used the Mosaic Analysis with a Repressible Cell Marker (MARCM) technique (Lee and Luo, 2001) to generate small number of homozygous ISCs and the subsequent lineages that were positively marked by GFP. We tested msn^{102} and msn^{172}, both of which are X-ray induced inversions and likely null alleles, as well as msn^{P06946}, a *P* element insertion allele (Braun et al., 1997; Horne-Badovinac et al., 2012; Ruan et al., 2002; Treisman et al., 1997). As shown in Fig. 2A–D and Fig. S2B, the number of GFP^+ cells in *msn* mutant clones of all three alleles was significantly higher than that in wild type clones.

The increase in cell number of *msn* mutant clones, however, is lower than anticipated considering the strong RNAi-induced phenotype. If *msn* is required within ISC, one should expect the null mutants have stronger proliferation phenotype than that in RNAi experiments. A logical explanation is that *msn* is required outside ISC but influences ISC division indirectly. The number of MARCM mutant cells in the above experiments was much smaller than that in the esg>RNAi experiment, therefore could result in weaker stimulation of overall midgut proliferation. To examine this further, we used additional drivers, the *Myo1A-Gal4*, *Su(H)-Gal4* or *Dl-Gal4* to induce msn^{RNAi} in ECs, EBs or ISCs, respectively (Jiang et al., 2009; Zeng et al., 2010). Within days of temperature shift, both *esg-Gal4* and *Su(H)-Gal4* drove a highly increased p-$H3^+$ cell count. *Myo1A-Gal4* and *Dl-Gal4* caused a much lower effect (Fig. 2F, G). The common cell type shared by the *esg* and *Su(H)* drivers is the EB, suggesting that Msn acts largely in EBs to increase ISC division. We then repeated the MARCM experiments with longer incubation time after clone induction to accumulate more mutant cells in the midgut. Under such experimental condition, we quantified the p-$H3^+$ cells inside and outside GFP^+ clusters and found that a large portion of the mitotic cells were outside the mutant clones (Fig. 2E), indicating that an ISC-non-autonomous mechanism takes place to induce proliferation of surrounding cells by the *msn* mutant cells.

We have examined the expression of the *msn-lacZ* insertion line msn^{P06946}, the same one we used in our mutant phenotypic analyses. Previous reports (Braun et al., 1997; Rudrapatna et al., 2013) used this line as a reporter for *msn* expression, so presumably it represents authentic expression. Our β-galactosidase antibody staining showed higher expression in enteroblasts, much lower in ISCs and not detectable in ECs (Fig. 2H–H′). This is consistent with the functional requirement in enteroblasts, although one cannot make a direct argument

between the level of expression and functional requirement especially for these kinases, which likely require phosphorylation for activation.

Pdm1 is a differentiation marker for mature ECs and late EBs (Zhou et al., 2013). In mutant *msn* MARCM clones, there was also Pdm1 staining in the bigger GFP^+ cells, similar to the ECs in surrounding and in control MARCM clones (Fig. 2I, J). In esg>msn^{RNAi} guts, many of the GFP^+ cells in the multi-layered epithelium stained positive for Pdm1 (Fig. 2K, L, arrowheads), and overlapped extensively with Su(H)lacZ expression (Fig. S2C). Moreover, we did not observe an abnormal increase of EEs based on the staining of Prospero (Pros) (Fig. S1D). These results demonstrate that loss of *msn* function leads to an increased ISC proliferation by a non-autonomous mechanism, followed by faster and largely normal differentiation, which are hallmarks of hyperplasia.

Upd3 is essential for ISC over-proliferation caused by loss of *msn*

A simple prediction based on the non-autonomous mechanism is that loss of Msn leads to the production of a growth factor to increase ISC proliferation. We assayed for the expression of ligands shown to be important for midgut growth by RT-PCR of RNA from midguts of the *esg*>msn^{RNAi} flies (Jiang et al., 2009; Ren et al., 2010). The results revealed that expression of the JAK-STAT pathway ligand *upd3* showed a particularly robust increase (Fig. 3A). A downstream target gene of the JAK-STAT pathway *Socs36E* also showed a significant increase in the expression (Fig. 3A).

To visualize the expression *in vivo*, we examined the 4 kb *upd3* promoter-*lacZ* reporter that expressed in both mature ECs and differentiating EBs (Jiang et al., 2009; Zhou et al., 2013). In wild type guts, this *lacZ* reporter largely had no expression but occasional low level staining (Fig. 3C, E). In *esg*>msn^{RNAi} guts, the GFP^+ cells almost all contained β-galactosidase protein staining, except some small cells that probably represented ISCs and early EBs (Fig. 3D, arrowheads). The *msn* mutant MARCM clones also exhibited strong correlation with increased *upd3-lacZ* expression (Fig. 3F). Quantification of the MARCM clones showed that only 6% of the wild type clones (n=83) had β-galactosidase co-staining, while 58% (n=264) of the mutant clones had extensive co-staining, with many of remaining mutant clones showing partial overlap with β-galactosidase staining. These results together demonstrate a negative regulation of *upd3* expression by Msn in the midgut.

Over-expression of Upd3 from midgut precursor cells driven by both *esg-Gal4* and *Su(H)-Gal4* caused highly increased ISC proliferation within 1–3 days (Fig. 3B). Therefore, the production of Upd3 from EBs is functionally relevant. Furthermore, the knockdown of *upd3* expression by using two different $upd3^{RNAi}$ constructs caused almost complete suppression of the midgut proliferation induced by *esg-Gal4* or *Su(H)-Gal4* driven msn^{RNAi} (Fig. 3G). The confocal images shown in Fig. 3H–J illustrate that in the double RNAi guts, fewer Su(H)>GFP^+ cells were present when compared to msn^{RNAi} alone and the multilayering of the midgut epithelium was also suppressed (Fig. 3K–M). These experiments together demonstrate that Upd3 is an important downstream effector for the increased ISC division and midgut hyperplasia phenotype.

Yorkie but not JNK is a critical mediator downstream of Msn

Misshapen regulates a number of biological processes including embryonic dorsal closure, axonal projection, planar cell polarity, egg chamber elongation and oocyte border cell migration (Cobreros-Reguera et al., 2010; Horne-Badovinac et al., 2012; Paricio et al., 1999; Ruan et al., 2002; Su et al., 1998; Treisman et al., 1997). JNK may act downstream of Msn in some of these processes. We tested the requirement of JNK in EBs. Three different dsRNA constructs driven by *Su(H)-Gal4* all caused moderate increase of ISC proliferation (Fig. 4A), which is opposite to JNK function described in midgut ECs as a positive regulator of stress-induced ISC proliferation and age-dependent intestinal dysplasia (Biteau et al., 2008; Jiang et al., 2009). Moreover, JNK silencing in EBs did not cause a significant increase of *upd3* mRNA and the proliferation phenotype was not suppressed by *upd3* RNAi, nor suppressed by *yki* RNAi (Fig. 4A). The JNK phosphorylation normally associated with the kinase activity had no detectable change after msn^{RNAi} (Fig. 4B). The inclusion of the anti-apoptotic protein p35 also did not suppress the msn^{RNAi}-induced phenotype (Fig. 4C). These results suggest that a change of JNK activity or death-related mechanism is not the underlying reason for the *msn*-dependent phenotype.

Previous reports have shown that damage-induced response in ECs can be regulated by Yki (Ren et al., 2010; Shaw et al., 2010; Staley and Irvine, 2010). When we tested the requirement in EBs, the result clearly indicated a critical function of Yki downstream of Msn. The double RNAi experiment caused almost complete suppression of the hyperplasia, ISC proliferation, and *upd3* and *Socs36E* expression phenotypes (Fig. 4D–K). This suppression by loss of Yki was observed by using either *esg* or *Su(H)* driver, demonstrating that both Msn and Yki are required in the same cell type, that is EB.

Msn interacts genetically with Warts and acts independently of Hpo

Msn and Hpo belong to different subfamilies of the GCK family of protein kinases (Strange et al., 2006). The highly conserved Hpo-Wts-Yki pathway, MST1/2-LATS-YAP in mammals, controls organ size by regulating the cell cycle and apoptosis (Harvey and Hariharan, 2012; Zhao et al., 2011). However, Hpo/MST are not required downstream of the F-actin cytoskeleton in mechanosensing and G-protein coupled receptor signaling where Yki/YAP are critical (Aragona et al., 2013; Sansores-Garcia et al., 2011; Yu et al., 2012). Therefore, a different kinase might act similarly to Hpo/MST in some processes.

We examined the relationship among Msn, Hpo and Wts in the adult midgut. For these experiments, we used *hpo*, *wts* and *msn* RNAi lines from VDRC. The EC driver *Myo1A-Gal4* with hpo^{RNAi} caused a substantial increase in midgut proliferation as previously reported (Ren et al., 2010; Shaw et al., 2010; Staley and Irvine, 2010), while with msn^{RNAi} had a weaker effect (Fig. 5A). The EB driver *Su(H)-Gal4* caused an opposite outcome, with msn^{RNAi} leading to a very high cell proliferation but hpo^{RNAi} having little if any effect (Fig. 5B). The *esg-Gal4* driver also caused stronger phenotype with msn^{RNAi} than with hpo^{RNAi}. The *Dl-Gal4* caused weak phenotype overall, likely due to a weak expression of this driver (Fig. 5C, D). The wts^{RNAi} phenotypes were always among the strongest with any of the drivers. These results together establish the scenario that Wts has an essential role in all cell types, while Msn is required in EB where Hpo does not appear to be critical.

We then tested the functional interaction among these kinases, all using the EB driver. First, the msn^{RNAi}-induced proliferation phenotype was efficiently rescued by two different *msn* cDNA constructs, while the inclusion of a *hpo* cDNA did not have significant rescue (Fig. 5E). Second, increased expression of *wts* by a transgene suppressed efficiently the msn^{RNAi}-induced proliferation phenotype (Fig. 5F). Third, the wts^{RNAi}-induced proliferation was similarly suppressed by loss of Yki function, and the *wts/+* heterozygous mutant significantly enhanced the msn^{RNAi}-induced proliferation phenotype (Fig. 5G). These results demonstrate that Hpo cannot replace Msn, while Msn and Wts act in parallel or together to regulate downstream events such as Yki function in EBs.

Physical interaction between Msn and Wts is conserved

Recent reports demonstrate that Wts interacts with Merlin, Hpo interacts with Salvador and Msn interacts with the membrane protein Fat (Kwon et al., 2013; Yin et al., 2013), suggesting a complex interaction among the components of this signaling pathway. We examined the physical interaction between Msn and Wts by transient transfection. The tagged versions of the constructs were transfected into S2 cells and the extracts then used for co-immunoprecipitation (IP). The results from reciprocal co-IP experiments showed that over-expressed Msn and Wts formed a complex in these extracts (Fig. 6A, B). A parallel experiment using mammalian HEK293 cells also showed that transfected mammalian Msn homolog MAP4K4 and Wts homolog LATS2 formed a complex under the co-IP condition (Fig. 6G).

We then tested whether Msn can affect the phosphorylation of Wts. Msn activity is increased after treatment of the cells with the phosphatase inhibitor okadaic acid (OA), probably due to activation of upstream events (Kaneko et al., 2011). OA treatment alone caused a slower mobility of Wts and the addition of Msn caused further retardation on SDS gels (Fig. 6C). This further mobility shift of Wts was not observed when the ATP binding site mutation K61R of Msn was used (Fig. 6D). Moreover, phosphatase treatment of the extracts abolished this shift (Fig. 6E), demonstrating that the cause of mobility shift of Wts was phosphorylation. As a comparison, Msn did not cause a detectable mobility shift of Hpo (Fig. 6F).

Activated Wts causes phosphorylation of Yki at the S168 residue, which inhibits Yki by causing its cytoplasmic retention. In our pilot experiments, co-transfection of Wts was sufficient to cause phosphorylation of Yki, to an extent that the addition of Msn did not make a difference. However, when lower amounts of Wts were used, Yki phosphorylation was not observed unless Msn was included (Fig. 6H). The K61R mutation on Msn again almost abolished this function.

Similarly, LATS phosphorylation at the S909 residue (autophosphorylation site) and T1079 residue (a known MST1/2 target site) were increased after co-transfection of MAP4K4 into HEK293 cells, while the ATP binding site mutant K54R of MAP4K4 did not cause such effects (Fig. 6I). In addition, wild type but not mutant MAP4K4 promoted phosphorylation of transfected YAP at the S127, a well-established target site of activated LATS.

To further demonstrate the *in vivo* relevance of MAP4K4 in regulating the pathway, we utilized mouse embryo fibroblasts, a cell type where the endogenous LATS and YAP are phosphorylated but somehow is not affected after MST1/2 double knockout (Song et al., 2010; Zhou et al., 2009). The knockout of MAP4K4 by inducible Cre-mediated recombination in these cells led to a reduction of LATS and YAP phosphorylation both before and after Latrunculin B treatment (Fig. 6J, K), which inhibits actin polymerization and increases YAP phosphorylation (Yin et al., 2013; Zhao et al., 2011). These results demonstrate that MAP4K4 is a critical component regulating LATS-YAP in this cell type and that the *Drosophila* Msn-Wts and mammalian MAP4K4-LATS interactions are conserved.

Functional interaction of Msn and Wts leads to inactivation of Yki

Yki is a transcription co-activator of Scalloped (Sd). A luciferase reporter with Sd binding sites has previously been shown to be activated by Yki-Sd, as well as repressed by Hpo-Wts (Zhang et al., 2008). We used this reporter because there is no other established reporter yet to assay for Msn repression. The co-transfection of Hpo, Wts or Msn individually could not repress the Yki-Sd-dependent expression of the reporter. The inclusion of Hpo and Wts together repressed approximately 50% of the expression, while Msn and Wts together repressed approximately 28% of the expression (Fig. 7A). The Msn K61R mutant did not show significant repression. Therefore, Msn and Wts can act synergistically to decrease the transcriptional activity of Yki.

To assay for a functional interaction between MAP4K4 and LATS-YAP, endogenous YAP localization was quantified in 293A cells because LATS phosphorylation of YAP results in YAP inhibition by translocation to the cytoplasm. Expressing a low level of LATS alone had a small effect while co-expression of LATS and MAP4K4 synergistically increased the number of cells with cytoplasmic accumulation of YAP (Fig. 7B–D), supporting our model of a conserved functional interaction.

The knockdown of actin capping protein A (Cpa), B (Cpb) or overexpression of the actin nucleation factor Diaphanous (Dia^{CA}) can cause extra actin polymerization and activation of Yki in *Drosophila* developing discs and S2 cells (Sansores-Garcia et al., 2011). By *Su(H)-Gal4* driven expression, we showed that these approaches caused a significant increase of midgut proliferation. This proliferation phenotype was efficiently suppressed by Msn overexpression, *upd3* RNAi or *yki* RNAi (Fig. 7E). Therefore, Msn together with Yki and Upd3 are critical components downstream of F-actin dynamics in EBs to control midgut homeostasis.

DISCUSSION

Previous studies have shown that ECs produce regulatory factors in response to infection and damage, and function as part of the niche to regulate ISC-mediated regeneration (Buchon et al., 2010; Jiang et al., 2009; Ren et al., 2010; Shaw et al., 2010; Staley and Irvine, 2010). Meanwhile, recent reports show that EBs can also produce growth factors including EGF receptor ligands, Wingless and Upd3, although the pathways that regulate their production are not known (Cordero et al., 2012; Jiang et al., 2010; Xu et al., 2011;

Zhou et al., 2013). Our results here demonstrate that differentiating EBs also function as an important part of the niche to regulate ISC division via the Msn pathway. EB-specific knockdown of *msn* leads to highly increased Upd3 expression and midgut proliferation (see Fig. 3). A previous report suggests that undifferentiated EBs if remain in contact with the mother ISC can inhibit proliferation (Choi et al., 2011). Although the hyperproliferating midguts after loss of Msn contain many EBs, these EBs do go into normal differentiation and express high level of Upd3, which may overcome any inhibitory effect of undifferentiated EBs on ISC proliferation.

Msn is known to regulate a number of biological processes (Cobreros-Reguera et al., 2010; Horne-Badovinac et al., 2012; Paricio et al., 1999; Ruan et al., 2002; Su et al., 1998; Treisman et al., 1997). During embryonic dorsal closure the MAP kinase pathway Slipper-Hemipterous-JNK is downstream of Msn, and Slipper is able to bind to Msn in vitro (Garlena et al., 2010). In the adult midgut, JNK is a mediator of aging-related intestinal dysplasia and is a stress-activated kinase in ECs to positively regulate ISC division (Biteau et al., 2008; Buchon et al., 2009; Jiang et al., 2009). While our RNAi experiments show that JNK has a function in EBs to negatively regulate ISC proliferation (see Fig. 4), this phenotype is not dependent on Upd3 or Yki. We also could not detect a change of JNK phosphorylation after loss of Msn. Mammalian MAP4K4 has also been shown to function independently of JNK in some biological contexts (Danai et al., 2013; Wang et al., 2012). Therefore, Msn and JNK probably have independent functions in the midgut.

We have instead uncovered a novel interaction of Msn with Wts and subsequently regulation of Yki. Hpo-Wts-Yki has been demonstrated to have a function in ECs for stress and damage-induced response (Karpowicz et al., 2010; Ren et al., 2010; Shaw et al., 2010; Staley and Irvine, 2010). Gal4 driven experiments have many caveats including cell type specificity, differences in promoter strengths, and knockdown efficiency in different cell types. Nonetheless, the results of many parallel experiments we conducted strongly suggest that Msn and Hpo independently regulate Wts-Yki in EBs and ECs, respectively (see Fig. 5). How the Msn and Hpo pathways in the two cell types are coordinately regulated to produce an appropriate amount of Upd3 to achieve desirable intestinal growth under different circumstances remains an important question to be answered.

Previous experiments in developing discs suggest that Wts and Yki but not Hpo act downstream of cytoskeleton regulators (Sansores-Garcia et al., 2011). Similarly, the mammalian Hpo homologs MST1/2 appear not to be involved in LATS regulation after cytoskeletal perturbation in some cell types (Zhao et al., 2012). Our in vivo assay in midgut suggests a function for Msn, Yki and Upd3 downstream of actin capping proteins in EBs (see Fig. 7). Similarly, the Latrunculin B effect on MEFs suggests that MAP4K4 is required for cytoskeleton-regulated LATS and YAP phosphorylation (Fig. 6). The situation in mammalian cells may be more complicated since the Msn/MAP4K4 subfamily also includes two other closely related kinases TNIK and MINK1 (Strange et al., 2006). Proper regulation of Wts by the cytoskeleton may require both positive and negative regulators, since recent work in flies identified the LIM-domain protein Jub as a negative regulator of Wts in response to cytoskeletal tension (Rauskolb et al., 2014). It will be interesting in future

studies to determine how positive and negative regulators of Wts act in a coordinated manner to regulate cell fate and proliferation in response to cytoskeletal tension.

EXPERIMENTAL PROCEDURES

Drosophila stocks and genetics

UAS-mCD8GFP and w^{1118} were used as wild type stocks for crossing with various Gal4 and mutant lines for control experiments. The transgenic RNAi fly stocks used are: *msn* (VDRC101517, TRiP28791), *upd3* (VDRC27136, TRiP28575), *yki* (TRiP31965), *hpo* (VDRC104169), JNK (VDRC34138, VDRC3139, VDRC104569, TRiP32977), cpa (VDRC100773), cpb (TRiP50954). The following stocks were obtained from Bloomington stock center: $FRT80Bmsn^{102}$ (5945), $FRT80Bmsn^{172}$ (5947), msn^{P06946} (6946), UAS-wts (44250), wts^{X-1} (44251), $Diaphanous^{CA}$ (27616). We generated the $FRT80Bmsn^{P06946}$ stock by meiotic recombination of the msn^{P06946} and wild type chromosome carrying *FRT80B* based on G418 selection. *esg-Gal4*, *Su(H)Gbe-Gal4*, *Myo1A-gal4*, *Dl-Gal4* and UAS-upd3 were as described (Jiang et al., 2009; Micchelli and Perrimon, 2006; Ohlstein and Spradling, 2006; Zeng et al., 2010). The *Su(H)Gbe-Gal4* line on 2^{nd} chromosome was used for all the experiments in this report. The 4 kb *upd3-lacZ* fly line was a generous gift from Hervé Agaisse (Zhou et al., 2013). Mutant clones were generated by mitotic recombination using MARCM technique (Amcheslavsky et al., 2009; Lee and Luo, 2001). The final cross and offspring were maintained at room temperature. To induce mutant clones, 5 days old flies were heat shocked at 37°C for 1 hour, performed twice within 1 day. The flies were then kept at 18°C and incubated for an additional 10 days before dissection. Transgenic flies were generated in the w^{1118} background by the Genetic Services (Cambridge, MA) and Rainbow Transgenic Flies, Inc. (Camarillo, CA).

Plasmid constructs

Constructs that expressed the HA-tagged Msn^{WT}, Msn^{K61R} and Msn^{768} were generated in pBS cloning vector as described (Kaneko et al., 2011) and then subcloned into the pUAST vector using the *EcoRI* and *XbaI* sites. The HA-MAP4K4 constructs were as described (Kaneko et al., 2011). The LATS and YAP transfection plasmids were as described (Paramasivam et al., 2011). Myc-Wts, FLAG-Hpo and HA-Yki constructs were as reported (Zhang et al., 2008).

Tissue culture, transfection, real-time qPCR

Drosophila S2 cells were cultured in Schneider media supplemented with 10% FBS and transfected with Effectene (Qiagen). 293 cells were cultured in DMEM supplemented with 10% FBS and transfected with Lipofectamine 2000 (Invitrogen) in Opti MEM Medium. Okadaic acid treatment experiment and msn^{RNAi} in S2 cells was as described previously (Kaneko et al., 2011). HA-tagged MAP4K4 or Msn immunoprecipitation were as described (Kaneko et al., 2011; Paramasivam et al., 2011). For real time quantitative PCR, total RNA was isolated from 10 dissected female guts and used to prepare cDNA. PCR was performed using iQ5 System (Bio-Rad). The sequences of primers used can be found in previous reports (Ren et al., 2010). The RT-qPCR was performed in duplicate from each of at least 3 independent biological samples. The *ribosomal protein 49* (*rp49*) gene was used as the

internal control for normalization of cycle number. Luciferase assay was as described (Zhang et al., 2008).

ES cells containing Map4k4 exon 7 flanked by loxP sites were obtained from Texas A&M institute for genomic medicine, and mice bearing the targeted allele were generated by blastocyst injection. The animals were backcrossed to C57Bl6/J mice for 6 generations before crossing to UBC-cre/ERT2 animals [Jackson Laboratories B6.Cg-Tg (UBC-cre/ERT2) 1Ejb/J]. Primary MEFs were derived from E12.5 embryos that were minced and incubated with trypsin/EDTA at 37°C for 30 min followed by mechanical disruption via pipetting. Isolated cells were cultured at 37°C, 5% CO_2 in DMEM supplemented with 10% FBS and 1% penicillin/streptomycin. MEFs were immortalized with SV40 T antigen and serial passages. MAP4K4 was deleted by incubation with 4-OH tamoxifen (Sigma H7904) (2.5 μM) in DMEM for 72 hours prior to experimentation.

Immunostaining, fluorescent microscopy and Western blot

Female flies were used for routine gut dissection, because of the bigger size, and staining and antibodies used were as described, except rabbit anti-p-H3 was from Millipore (1:1000 dilution) (Amcheslavsky et al., 2009). Microscope image acquisition and processing was as described (Amcheslavsky et al., 2011). Western blots were performed as described (Kaneko et al., 2011; Paramasivam et al., 2011). The antibodies used for Western blots and cell staining were: LATS (Bethyl A300-479A), phospho-LATS Thr1079 (Cell signaling #8654), phospho-LATS S909 (Cell signaling #9157), YAP (Santa Cruz sc-15407 rabbit and sc-101199 mouse), Phospho-YAP (Cell signaling #4911), HA (Covance 16B12), HA (Santa Cruz sc-805), FLAG (Sigma M2 F1804), Myc (Santa Cruz sc-46, 9E10), p-JNK (Cell signaling #9251), MAP4K4 (Bethyl A301-503A), E-cadherin (Hybridoma bank). The Yki-S168 and Yki antibodies were generous gifts from Dr. D. Pan (Johns Hopkins U.).

Supplementary Material

Refer to Web version on PubMed Central for supplementary material.

Acknowledgments

We acknowledge the Vienna *Drosophila* RNAi Center and the Bloomington *Drosophila* Stock Center for the transgenic RNAi lines. We thank Drs. Hervé Agaisse, DJ Pan, Huaqi Jiang, Steven Hou, Jianghang Jia, Lei Zhang and Xiaohang Yang for fly stocks and reagents. YTI is supported by an NIH grant (DK83450), is a member of the UMass DERC (DK32520), a member of the UMass Center for Clinical and Translational Science (UL1TR000161), and a member of the Guangdong Innovative Research Team Program (No. 201001Y0104789252). JM is supported by an American Cancer Society grant (120376-RSG-11-040-01-DDC). JJ is supported by NIH grants (GM61269 and GM67045), a CPRIT grant (RP130542), a Welch foundation grant (I-1603), and a NSFC (31328017). These studies were also supported by grants to MPC from the National Institutes of Health (DK030898) and the International Research Alliance of the Novo Nordisk Foundation Center for Metabolic Research. DM was supported by National Institutes of Health grant GM058406-14.

References

Amcheslavsky A, Ito N, Jiang J, Ip YT. Tuberous sclerosis complex and Myc coordinate the growth and division of Drosophila intestinal stem cells. J Cell Biol. 2011; 193:695–710. [PubMed: 21555458]

Amcheslavsky A, Jiang J, Ip YT. Tissue damage-induced intestinal stem cell division in Drosophila. Cell Stem Cell. 2009; 4:49–61. [PubMed: 19128792]

Aragona M, Panciera T, Manfrin A, Giulitti S, Michielin F, Elvassore N, Dupont S, Piccolo S. A mechanical checkpoint controls multicellular growth through YAP/TAZ regulation by actin-processing factors. Cell. 2013; 154:1047–1059. [PubMed: 23954413]

Barker N, van Es JH, Kuipers J, Kujala P, van den Born M, Cozijnsen M, Haegebarth A, Korving J, Begthel H, Peters PJ, et al. Identification of stem cells in small intestine and colon by marker gene Lgr5. Nature. 2007; 449:1003–1007. [PubMed: 17934449]

Beebe K, Lee WC, Micchelli CA. JAK/STAT signaling coordinates stem cell proliferation and multilineage differentiation in the Drosophila intestinal stem cell lineage. Dev Biol. 2010; 338:28–37. [PubMed: 19896937]

Biteau B, Hochmuth CE, Jasper H. JNK activity in somatic stem cells causes loss of tissue homeostasis in the aging Drosophila gut. Cell Stem Cell. 2008; 3:442–455. [PubMed: 18940735]

Biteau B, Jasper H. EGF signaling regulates the proliferation of intestinal stem cells in Drosophila. Development. 2011; 138:1045–1055. [PubMed: 21307097]

Bond D, Foley E. Autocrine platelet-derived growth factor-vascular endothelial growth factor receptor-related (Pvr) pathway activity controls intestinal stem cell proliferation in the adult Drosophila midgut. J Biol Chem. 2012; 287:27359–27370. [PubMed: 22722927]

Braun A, Lemaitre B, Lanot R, Zachary D, Meister M. Drosophila immunity: analysis of larval hemocytes by P-element-mediated enhancer trap. Genetics. 1997; 147:623–634. [PubMed: 9335599]

Buchon N, Broderick NA, Kuraishi T, Lemaitre B. Drosophila EGFR pathway coordinates stem cell proliferation and gut remodeling following infection. BMC Biol. 2010; 8:152. [PubMed: 21176204]

Buchon N, Broderick NA, Poidevin M, Pradervand S, Lemaitre B. Drosophila intestinal response to bacterial infection: activation of host defense and stem cell proliferation. Cell Host Microbe. 2009; 5:200–211. [PubMed: 19218090]

Choi NH, Kim JG, Yang DJ, Kim YS, Yoo MA. Age-related changes in Drosophila midgut are associated with PVF2, a PDGF/VEGF-like growth factor. Aging Cell. 2008; 7:318–334. [PubMed: 18284659]

Choi NH, Lucchetta E, Ohlstein B. Nonautonomous regulation of Drosophila midgut stem cell proliferation by the insulin-signaling pathway. Proc Natl Acad Sci U S A. 2011; 108:18702–18707. [PubMed: 22049341]

Cobreros-Reguera L, Fernandez-Minan A, Fernandez-Espartero CH, Lopez-Schier H, Gonzalez-Reyes A, Martin-Bermudo MD. The Ste20 kinase misshapen is essential for the invasive behaviour of ovarian epithelial cells in Drosophila. EMBO Rep. 2010; 11:943–949. [PubMed: 21102643]

Cordero JB, Stefanatos RK, Scopelliti A, Vidal M, Sansom OJ. Inducible progenitor-derived Wingless regulates adult midgut regeneration in Drosophila. EMBO J. 2012; 31:3901–3917. [PubMed: 22948071]

Danai LV, Guilherme A, Guntur KV, Straubhaar J, Nicoloro SM, Czech MP. Map4k4 suppresses Srebp-1 and adipocyte lipogenesis independent of JNK signaling. J Lipid Res. 2013; 54:2697–2707. [PubMed: 23924694]

de Navascues J, Perdigoto CN, Bian Y, Schneider MH, Bardin AJ, Martinez-Arias A, Simons BD. Drosophila midgut homeostasis involves neutral competition between symmetrically dividing intestinal stem cells. EMBO J. 2012; 31:2473–2485. [PubMed: 22522699]

Garlena RA, Gonda RL, Green AB, Pileggi RM, Stronach B. Regulation of mixed-lineage kinase activation in JNK-dependent morphogenesis. J Cell Sci. 2010; 123:3177–3188. [PubMed: 20736302]

Goulas S, Conder R, Knoblich JA. The Par complex and integrins direct asymmetric cell division in adult intestinal stem cells. Cell Stem Cell. 2012; 11:529–540. [PubMed: 23040479]

Grompe M. Tissue stem cells: new tools and functional diversity. Cell Stem Cell. 2012; 10:685–689. [PubMed: 22704508]

Guo Z, Driver I, Ohlstein B. Injury-induced BMP signaling negatively regulates Drosophila midgut homeostasis. J Cell Biol. 2013; 201:945–961. [PubMed: 23733344]

Harvey KF, Hariharan IK. The hippo pathway. Cold Spring Harb Perspect Biol. 2012; 4:a011288. [PubMed: 22745287]

Hochmuth CE, Biteau B, Bohmann D, Jasper H. Redox regulation by Keap1 and Nrf2 controls intestinal stem cell proliferation in Drosophila. Cell Stem Cell. 2011; 8:188–199. [PubMed: 21295275]

Horne-Badovinac S, Hill J, Gerlach G 2nd, Menegas W, Bilder D. A screen for round egg mutants in Drosophila identifies tricornered, furry, and misshapen as regulators of egg chamber elongation. G3 (Bethesda). 2012; 2:371–378. [PubMed: 22413091]

Huang H, Li J, Hu L, Ge L, Ji H, Zhao Y, Zhang L. Bantam is essential for Drosophila intestinal stem cell proliferation in response to Hippo signaling. Dev Biol. 2014; 385:211–219. [PubMed: 24262985]

Jiang H, Grenley MO, Bravo MJ, Blumhagen RZ, Edgar BA. EGFR/Ras/MAPK signaling mediates adult midgut epithelial homeostasis and regeneration in Drosophila. Cell Stem Cell. 2010; 8:84–95. [PubMed: 21167805]

Jiang H, Patel PH, Kohlmaier A, Grenley MO, McEwen DG, Edgar BA. Cytokine/Jak/Stat signaling mediates regeneration and homeostasis in the Drosophila midgut. Cell. 2009; 137:1343–1355. [PubMed: 19563763]

Kaneko S, Chen X, Lu P, Yao X, Wright TG, Rajurkar M, Kariya K, Mao J, Ip YT, Xu L. Smad inhibition by the Ste20 kinase Misshapen. Proc Natl Acad Sci U S A. 2011; 108:11127–11132. [PubMed: 21690388]

Kapuria S, Karpac J, Biteau B, Hwangbo D, Jasper H. Notch-Mediated Suppression of TSC2 Expression Regulates Cell Differentiation in the Drosophila Intestinal Stem Cell Lineage. PLoS Genet. 2012; 8:e1003045. [PubMed: 23144631]

Karpowicz P, Perez J, Perrimon N. The Hippo tumor suppressor pathway regulates intestinal stem cell regeneration. Development. 2010; 137:4135–4145. [PubMed: 21098564]

Kwon Y, Vinayagam A, Sun X, Dephoure N, Gygi SP, Hong P, Perrimon N. The Hippo signaling pathway interactome. Science. 2013; 342:737–740. [PubMed: 24114784]

Lee T, Luo L. Mosaic analysis with a repressible cell marker (MARCM) for Drosophila neural development. Trends Neurosci. 2001; 24:251–254. [PubMed: 11311363]

Li H, Qi Y, Jasper H. Dpp signaling determines regional stem cell identity in the regenerating adult Drosophila gastrointestinal tract. Cell Rep. 2013a; 4:10–18. [PubMed: 23810561]

Li Z, Zhang Y, Han L, Shi L, Lin X. Trachea-derived dpp controls adult midgut homeostasis in Drosophila. Dev Cell. 2013b; 24:133–143. [PubMed: 23369712]

Lin G, Xu N, Xi R. Paracrine Wingless signalling controls self-renewal of Drosophila intestinal stem cells. Nature. 2008; 455:1119–1123. [PubMed: 18806781]

Liu W, Singh SR, Hou SX. JAK-STAT is restrained by Notch to control cell proliferation of the Drosophila intestinal stem cells. J Cell Biochem. 2010; 109:992–999. [PubMed: 20082318]

Micchelli CA, Perrimon N. Evidence that stem cells reside in the adult Drosophila midgut epithelium. Nature. 2006; 439:475–479. [PubMed: 16340959]

O'Brien LE, Soliman SS, Li X, Bilder D. Altered modes of stem cell division drive adaptive intestinal growth. Cell. 2011; 147:603–614. [PubMed: 22036568]

Ohlstein B, Spradling A. The adult Drosophila posterior midgut is maintained by pluripotent stem cells. Nature. 2006; 439:470–474. [PubMed: 16340960]

Ohlstein B, Spradling A. Multipotent Drosophila intestinal stem cells specify daughter cell fates by differential notch signaling. Science. 2007; 315:988–992. [PubMed: 17303754]

Paramasivam M, Sarkeshik A, Yates JR 3rd, Fernandes MJ, McCollum D. Angiomotin family proteins are novel activators of the LATS2 kinase tumor suppressor. Mol Biol Cell. 2011; 22:3725–3733. [PubMed: 21832154]

Paricio N, Feiguin F, Boutros M, Eaton S, Mlodzik M. The Drosophila STE20-like kinase misshapen is required downstream of the Frizzled receptor in planar polarity signaling. EMBO J. 1999; 18:4669–4678. [PubMed: 10469646]

Perdigoto CN, Schweisguth F, Bardin AJ. Distinct levels of Notch activity for commitment and terminal differentiation of stem cells in the adult fly intestine. Development. 2011; 138:4585–4595. [PubMed: 21965616]

Ragab A, Buechling T, Gesellchen V, Spirohn K, Boettcher AL, Boutros M. Drosophila Ras/MAPK signalling regulates innate immune responses in immune and intestinal stem cells. EMBO J. 2011; 30:1123–1136. [PubMed: 21297578]

Rauskolb C, Sun S, Sun G, Pan Y, Irvine KD. Cytoskeletal tension inhibits Hippo signaling through an Ajuba-Warts complex. Cell. 2014; 158:143–156. [PubMed: 24995985]

Ren F, Shi Q, Chen Y, Jiang A, Ip YT, Jiang H, Jiang J. Drosophila Myc integrates multiple signaling pathways to regulate intestinal stem cell proliferation during midgut regeneration. Cell Res. 2013; 23:1133–1146. [PubMed: 23896988]

Ren F, Wang B, Yue T, Yun EY, Ip YT, Jiang J. Hippo signaling regulates Drosophila intestine stem cell proliferation through multiple pathways. Proc Natl Acad Sci U S A. 2010; 107:21064–21069. [PubMed: 21078993]

Ruan W, Long H, Vuong DH, Rao Y. Bifocal is a downstream target of the Ste20-like serine/threonine kinase misshapen in regulating photoreceptor growth cone targeting in Drosophila. Neuron. 2002; 36:831–842. [PubMed: 12467587]

Rudrapatna VA, Bangi E, Cagan RL. Caspase signalling in the absence of apoptosis drives Jnk-dependent invasion. EMBO Rep. 2013; 14:172–177. [PubMed: 23306653]

Sangiorgi E, Capecchi MR. Bmi1 is expressed in vivo in intestinal stem cells. Nat Genet. 2008; 40:915–920. [PubMed: 18536716]

Sansores-Garcia L, Bossuyt W, Wada K, Yonemura S, Tao C, Sasaki H, Halder G. Modulating F-actin organization induces organ growth by affecting the Hippo pathway. EMBO J. 2011; 30:2325–2335. [PubMed: 21556047]

Shaw RL, Kohlmaier A, Polesello C, Veelken C, Edgar BA, Tapon N. The Hippo pathway regulates intestinal stem cell proliferation during Drosophila adult midgut regeneration. Development. 2010; 137:4147–4158. [PubMed: 21068063]

Song H, Mak KK, Topol L, Yun K, Hu J, Garrett L, Chen Y, Park O, Chang J, Simpson RM, et al. Mammalian Mst1 and Mst2 kinases play essential roles in organ size control and tumor suppression. Proc Natl Acad Sci U S A. 2010; 107:1431–1436. [PubMed: 20080598]

Staley BK, Irvine KD. Warts and Yorkie mediate intestinal regeneration by influencing stem cell proliferation. Curr Biol. 2010; 20:1580–1587. [PubMed: 20727758]

Strange K, Denton J, Nehrke K. Ste20-type kinases: evolutionarily conserved regulators of ion transport and cell volume. Physiology (Bethesda). 2006; 21:61–68. [PubMed: 16443823]

Su YC, Treisman JE, Skolnik EY. The Drosophila Ste20-related kinase misshapen is required for embryonic dorsal closure and acts through a JNK MAPK module on an evolutionarily conserved signaling pathway. Genes Dev. 1998; 12:2371–2380. [PubMed: 9694801]

Takeda N, Jain R, LeBoeuf MR, Wang Q, Lu MM, Epstein JA. Interconversion between intestinal stem cell populations in distinct niches. Science. 2011; 334:1420–1424. [PubMed: 22075725]

Tan DW, Barker N. Intestinal stem cells and their defining niche. Curr Top Dev Biol. 2014; 107:77–107. [PubMed: 24439803]

Tian A, Jiang J. Intestinal epithelium-drived BMP controls stem cell self-renewal in Drosophila adult midgut. Elife. 2014; 3:e01857. [PubMed: 24618900]

Tian H, Biehs B, Warming S, Leong KG, Rangell L, Klein OD, de Sauvage FJ. A reserve stem cell population in small intestine renders Lgr5-positive cells dispensable. Nature. 2011; 478:255–259. [PubMed: 21927002]

Treisman JE, Ito N, Rubin GM. misshapen encodes a protein kinase involved in cell shape control in Drosophila. Gene. 1997; 186:119–125. [PubMed: 9047354]

Wang M, Amano SU, Roth Flach RJ, Chawla A, Aouadi M, Czech MP. Identification of Map4k4 as a novel suppressor of skeletal muscle differentiation. Mol Cell Biol. 2012

Xu N, Wang SQ, Tan D, Gao Y, Lin G, Xi R. EGFR, Wingless and JAK/STAT signaling cooperatively maintain Drosophila intestinal stem cells. Dev Biol. 2011; 354:31–43. [PubMed: 21440535]

Yan KS, Chia LA, Li X, Ootani A, Su J, Lee JY, Su N, Luo Y, Heilshorn SC, Amieva MR, et al. The intestinal stem cell markers Bmi1 and Lgr5 identify two functionally distinct populations. Proc Natl Acad Sci U S A. 2012; 109:466–471. [PubMed: 22190486]

Yin F, Yu J, Zheng Y, Chen Q, Zhang N, Pan D. Spatial organization of Hippo signaling at the plasma membrane mediated by the tumor suppressor Merlin/NF2. Cell. 2013; 154:1342–1355. [PubMed: 24012335]

Yu FX, Zhao B, Panupinthu N, Jewell JL, Lian I, Wang LH, Zhao J, Yuan H, Tumaneng K, Li H, et al. Regulation of the Hippo-YAP pathway by G-protein-coupled receptor signaling. Cell. 2012; 150:780–791. [PubMed: 22863277]

Zeng X, Chauhan C, Hou SX. Characterization of midgut stem cell- and enteroblast-specific Gal4 lines in drosophila. Genesis. 2010; 48:607–611. [PubMed: 20681020]

Zhang L, Ren F, Zhang Q, Chen Y, Wang B, Jiang J. The TEAD/TEF family of transcription factor Scalloped mediates Hippo signaling in organ size control. Dev Cell. 2008; 14:377–387. [PubMed: 18258485]

Zhao B, Li L, Wang L, Wang CY, Yu J, Guan KL. Cell detachment activates the Hippo pathway via cytoskeleton reorganization to induce anoikis. Genes Dev. 2012; 26:54–68. [PubMed: 22215811]

Zhao B, Tumaneng K, Guan KL. The Hippo pathway in organ size control, tissue regeneration and stem cell self-renewal. Nat Cell Biol. 2011; 13:877–883. [PubMed: 21808241]

Zhou D, Conrad C, Xia F, Park JS, Payer B, Yin Y, Lauwers GY, Thasler W, Lee JT, Avruch J, et al. Mst1 and Mst2 maintain hepatocyte quiescence and suppress hepatocellular carcinoma development through inactivation of the Yap1 oncogene. Cancer Cell. 2009; 16:425–438. [PubMed: 19878874]

Zhou F, Rasmussen A, Lee S, Agaisse H. The UPD3 cytokine couples environmental challenge and intestinal stem cell division through modulation of JAK/STAT signaling in the stem cell microenvironment. Dev Biol. 2013

Zhu L, Gibson P, Currle DS, Tong Y, Richardson RJ, Bayazitov IT, Poppleton H, Zakharenko S, Ellison DW, Gilbertson RJ. Prominin 1 marks intestinal stem cells that are susceptible to neoplastic transformation. Nature. 2009; 457:603–607. [PubMed: 19092805]

Zielke N, Korzelius J, van Straaten M, Bender K, Schuhknecht GF, Dutta D, Xiang J, Edgar BA. Fly-FUCCI: A versatile tool for studying cell proliferation in complex tissues. Cell Rep. 2014; 7:588–598. [PubMed: 24726363]

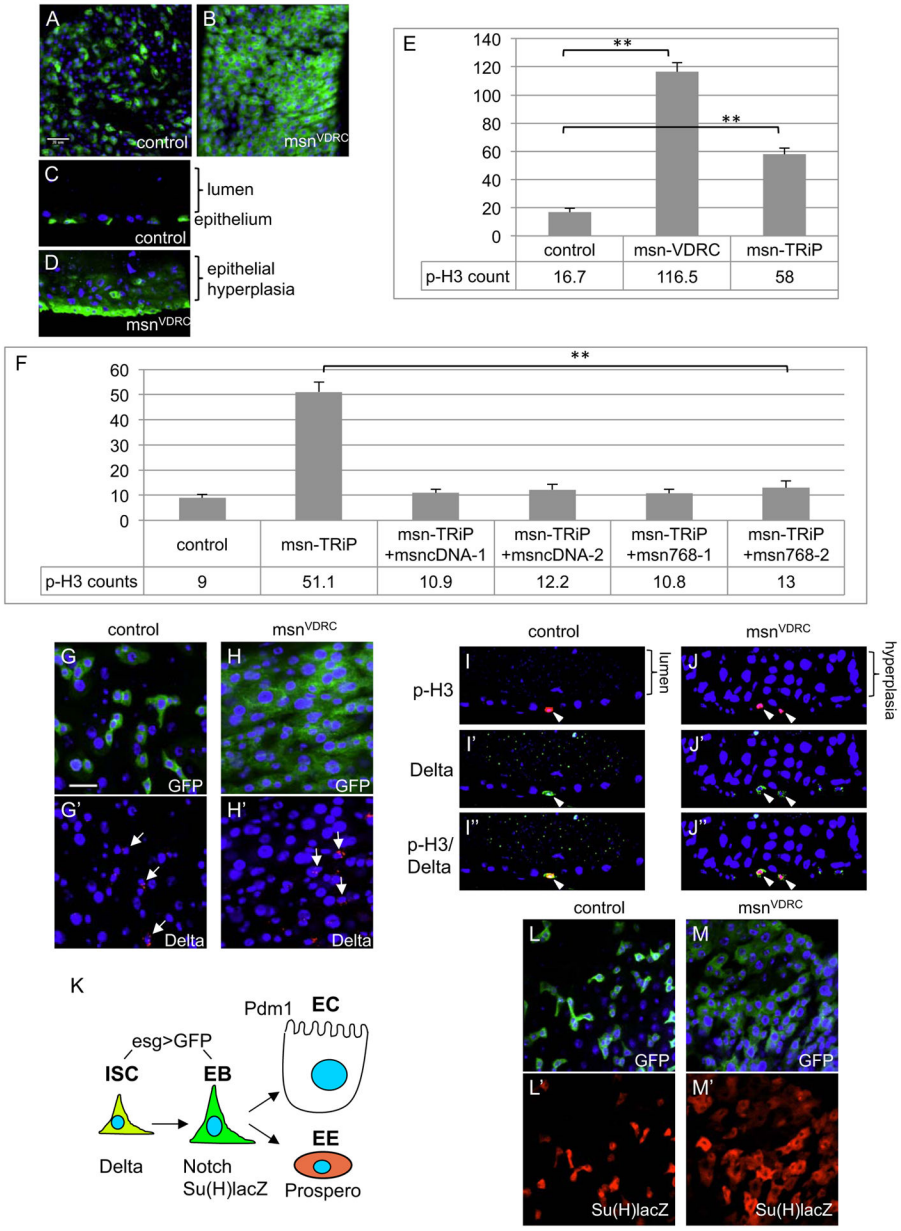

Figure 1. Loss of Msn causes midgut hyperplasia

(A–D) Confocal images of adult midguts. Panels B and C are surface views and panels D and E are sagittal views. Control gut is esg^{ts}>GFP, and msn^{RNAi} is esg^{ts}>GFP, UAS-msn$^{VDRC\text{-}RNAi}$. The flies were shifted to 29°C for 5 days to inactivate Gal80 and allow Gal4 activation. Green is GFP. For all panels in this report, blue is DAPI staining, scale bar is 20 μm and apical/lumen side is up for sagittal views. (E) Average number of p-H3^{+} cells per whole midgut of control (esg^{ts}>GFP) and msn^{RNAi} lines. The VDRC line consistently gave a stronger phenotype than that of the TRiP line. For all statistics in this report, the error bar is standard error of the mean unless indicated, and p value is from Student's T-test, ** is $p<0.01$. (F) Two independent transgenic lines of fully length *msn* cDNA and C-terminal truncation at amino acid 768 were crossed with the RNAi line and tested for rescue. The p

values were all <0.01 for the rescued lines compared to msn^{TRiP}. (G, H) Confocal images showing surface views of midguts. The msn^{VDRC} line was used for these the experiments, the esg^{ts}>GFP was used as driver and control, and temperature shift was carried out for 5 days. The arrows indicate some of the cells with cytoplasmic Delta staining (red). (I, J) Sagittal views confocal images of midguts. Nuclear p-H3 staining is red and cytoplasmic Delta staining is green. Cells that show both staining are ISCs in mitosis (arrowheads). (K) Schematic representation of the cell types and markers in the adult midgut. ISC, intestinal stem cell; EB, enteroblast; EC, enterocyte; EE, enteroendocrine cell. (L, M) Same RNAi experiments were performed but the lines also contained the Su(H)lacZ reporter chromosome. The β-galactosidase protein staining (red) from the reporter gene expression marks the EBs.

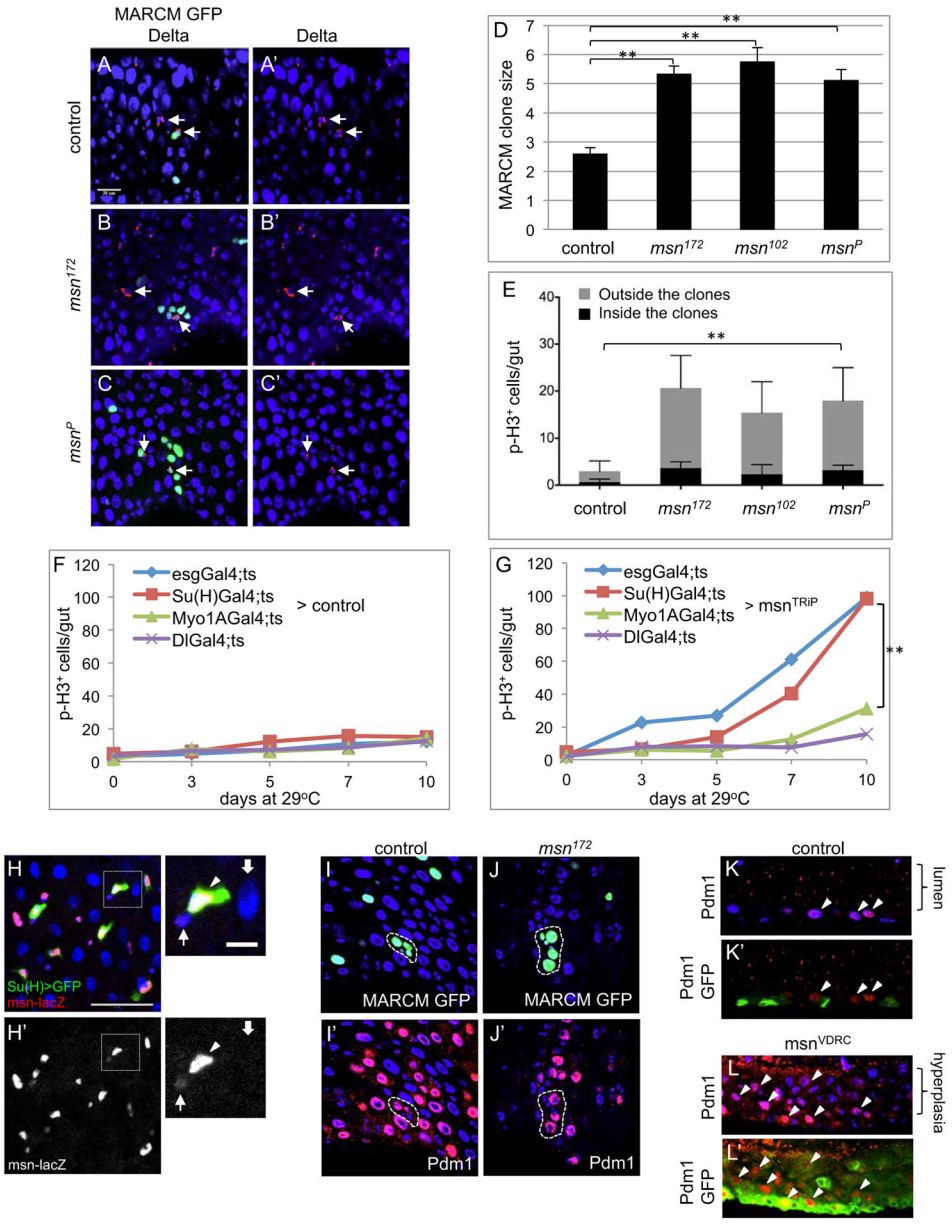

Figure 2. Msn functions in EBs to regulate ISC division non-autonomously

(A–C) Representative confocal images of MARCM clones. Cytoplasmic punctate Delta protein staining is red (arrows) and the MARCM nuclear GFP is green. Most GFP clusters each contained one Delta$^+$ cell. For clusters that contained two well-separated Delta$^+$ cells, the GFP$^+$ cell numbers were divided by two. (D) The average GFP$^+$ cell number per MARCM cluster in each homozygous genetic background is shown. Guts were dissected after 10 days incubation at 18°C after clone induction. (E) MRACM clone inductions were performed and the flies were incubated at 25°C for 7 days to accumulate more GFP$^+$ cells in the midgut. Guts were dissected and p-H3$^+$ cells inside and outside the GFP$^+$ clusters were quantified and the average number of each set was plotted as shown. The P value was calculated for total p-H3$^+$ cells of each mutant sample compared to control. (F, G) The

average number of p-H3^{+} cells of whole midguts in control (UAS-mCD8GFP) and UAS-msn^{TRiP} after crossing with the various drivers. The temperature shift to 29°C was carried out and at the days indicated a portion of the flies were used for midgut dissection and p-H3 staining. The p value in panel G is between the day 10 samples of Su(H)>msn^{TRiP} and Myo1A>msn^{TRiP}. (H) Confocal images of antibody staining for β-galactosidase expression in the midgut of *msn*^{P06946}, which was also crossed to contain the Su(H)Gal4 and UAS-GFP chromosomes. In the enlarged views of the white square area, the arrow indicates ISC, the arrowhead indicates EB, and the wide arrow indicates EC. (I, J) The MARCM clones (encircled) expressing nuclear GFP (green) or staining for the nuclear Pdm1 protein (nuclear red staining/purple color together with blue DAPI). (K, L) Sagittal view confocal images of midguts from control and *msn*^{VDRC} flies. Some of the Pdm1 stained nuclei are indicated by the arrowheads. Control gut is esg^{ts}>GFP. The flies were shifted to 29°C for 5 days.

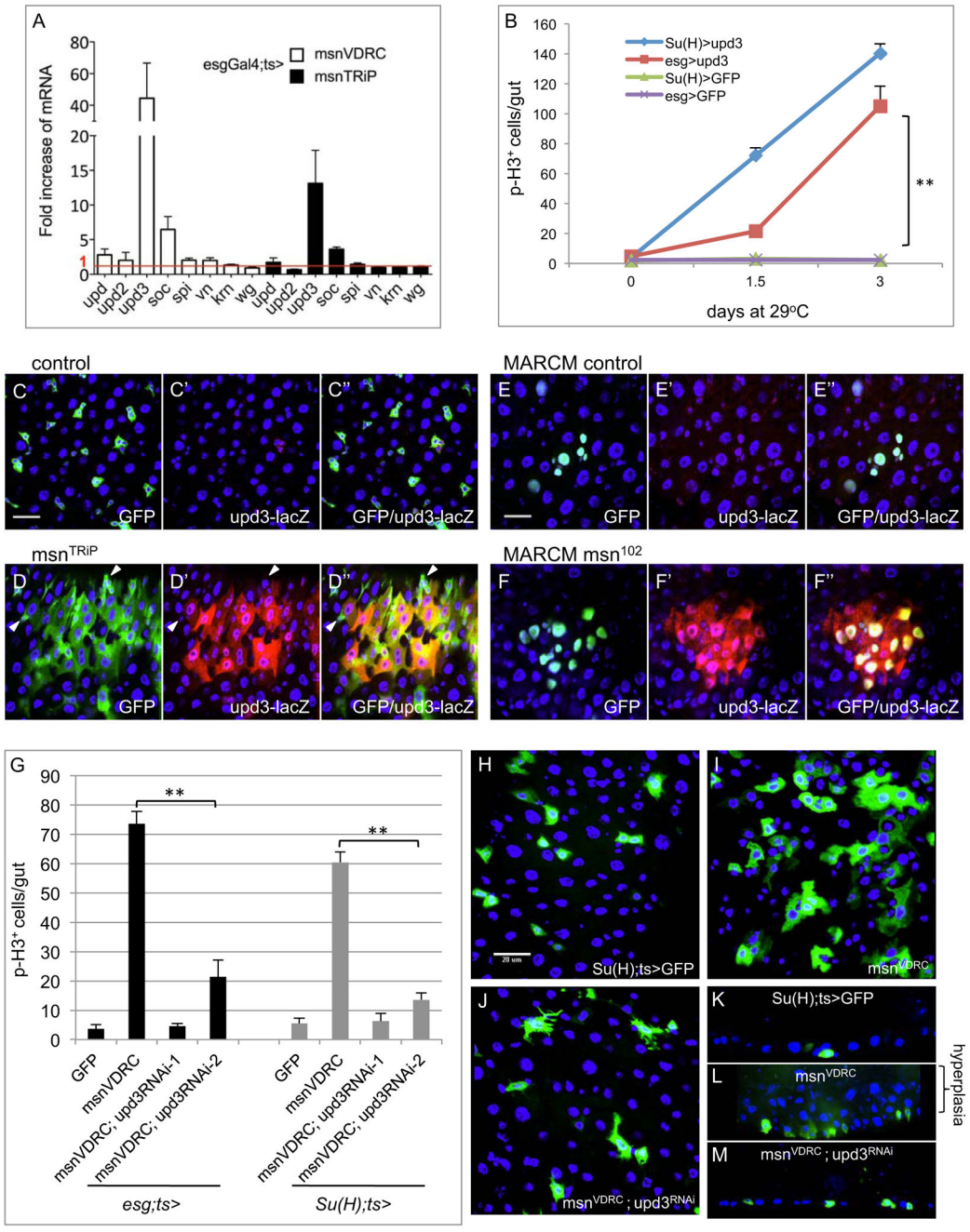

Figure 3. Upd3 is essential for the loss of *msn*-induced over-proliferation phenotype

(A) Relative mRNA expression for various growth factors. Control flies were esg^{ts}>GFP and the temperature shift was carried out for 3 days. Approximately 10 midguts form each sample were used for RNA isolation and RT-PCR. The cycle number of each PCR was normalized with that of the *rp49* in a parallel PCR. The normalized expression of the gene was divided by that of the GFP control and plotted as fold change. (B) Su(H)^{ts}> and esg^{ts}> were used to drive a UAS-upd3 cDNA or UAS-mCD8GFP as control. Whole guts were dissected after temperature shift for the indicated time and assayed for p-H3 count. The p

value is between esg^{ts}>upd3 and esg^{ts}>GFP. (C-F) The 4 kb *upd3* promoter-lacZ reporter was crossed together with the *msn* RNAi or mutant chromosomes. Panels C and D are control and *msn*^{RNAi} experiments using the esg^{ts}>GFP driver and temperature shift was for 3 days. The dissected guts were stained using an antibody for the β-galactosidase protein (red) and labeled as upd3-lacZ on the panel. Panels E and F are MARCM experiments. After heat shock induction the flies were incubated at 18°C for 10 days before gut dissection and stained for the β-galactosidase protein. (G) The single and double RNAi experiments were performed using the Su(H)^{ts}> and esg^{ts}> drivers. The flies were incubated at 29°C for 5 days and the gut assayed for the p-H3 count. Two different *upd3* RNAi lines were used. (H–J) The confocal images of midgut cells from Su(H)^{ts}>GFP^{+} or with the indicated RNAi lines are shown. (K–M) Sagittal view confocal images of midguts with the same genotypes.

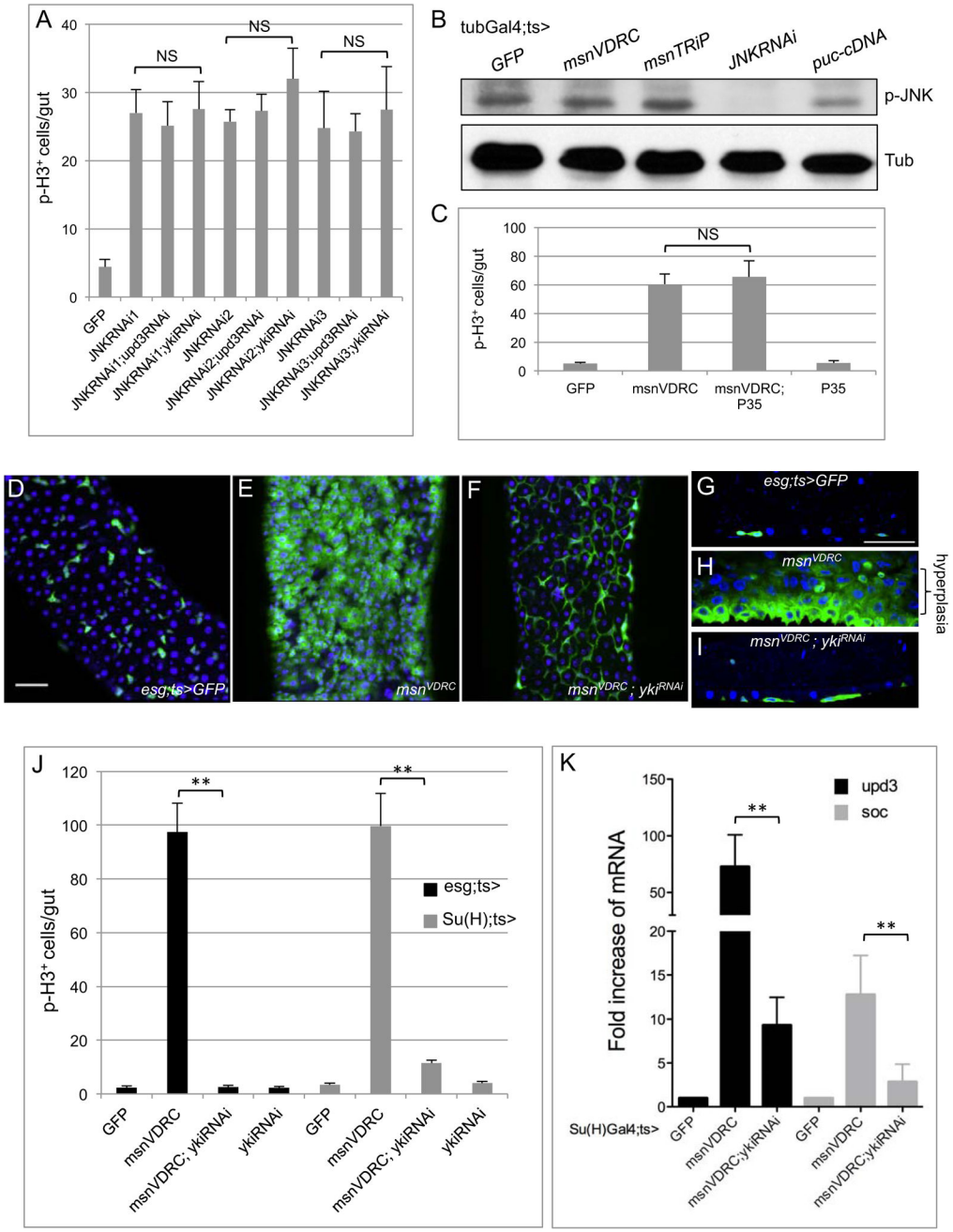

Figure 4. Yorkie but not JNK is a critical regulator downstream of Msn

(A) Su(H)Gal4^{ts} was used as the driver for these experiments. Midguts were dissected after 5 days at 29°C and the pH3 staining was counted. Three different JNK RNAi lines gave increased mitotic count, but none of them was suppressed by the double *yki* RNAi or *upd3* RNAi. NS is no significance with p>0.05. (B) Western blots of extracts from midguts of flies containing the indicated transgenes. Phospho-JNK and tubulin antibodies were used for the blots as indicated. Puckered (puc) is a JNK phosphatase. (C) The anti-apoptotic protein P35 was expressed using a transgenic cDNA construct. Su(H)Gal4^{ts} was used and temperature shift at 29°C was carried out for 5 days. (D–F) Confocal images of midguts

from flies with the indicated genotypes. The scale bar in panel D is 10 μm. (G–I) Sagittal view confocal images of midguts with the same genotypes. (J, K) The Gal4 drivers used are as indicated. The time at 29°C was 5 days for all these experiments. The p-H3 count is plotted in panel J. The fold change of mRNA expression by PCR in panel K was calculated by comparing to the control/GFP line as described in Fig. 3A.

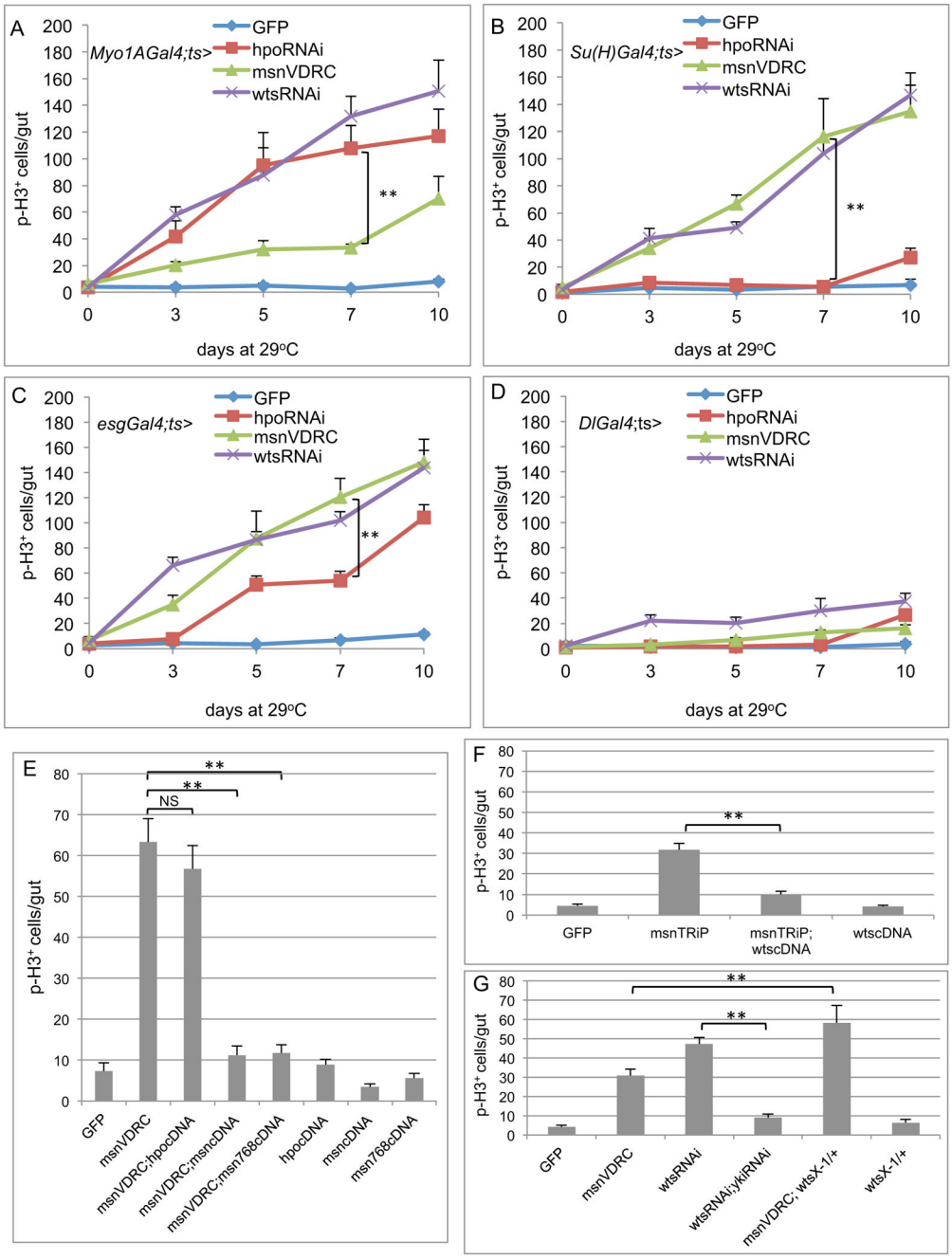

Figure 5. Msn interacts genetically with Warts and acts independently of Hippo

(AD) Midguts dissected from the RNAi lines with the indicated drivers were used for p-H3 staining and quantification. All crosses included the Gal80^{ts} and temperature shift to 29°C was carried out for 0–10 days as indicated. (E) The experiments were performed by using the Su(H)Gal4^{ts} and the shift to 29°C was for 5 days. The p-H3 staining was counted from midguts of flies with the indicated combination of *msn* RNAi and cDNA constructs. (F) Similar experiments using the combination of a *wts* cDNA were carried out. (G) Similar experiments were carried out to test the *yki* RNAi suppression of *wts* RNAi-induced

proliferation. The *msn* RNAi was also crossed together with a *wts/+* heterozygous background and tested for the proliferation phenotype.

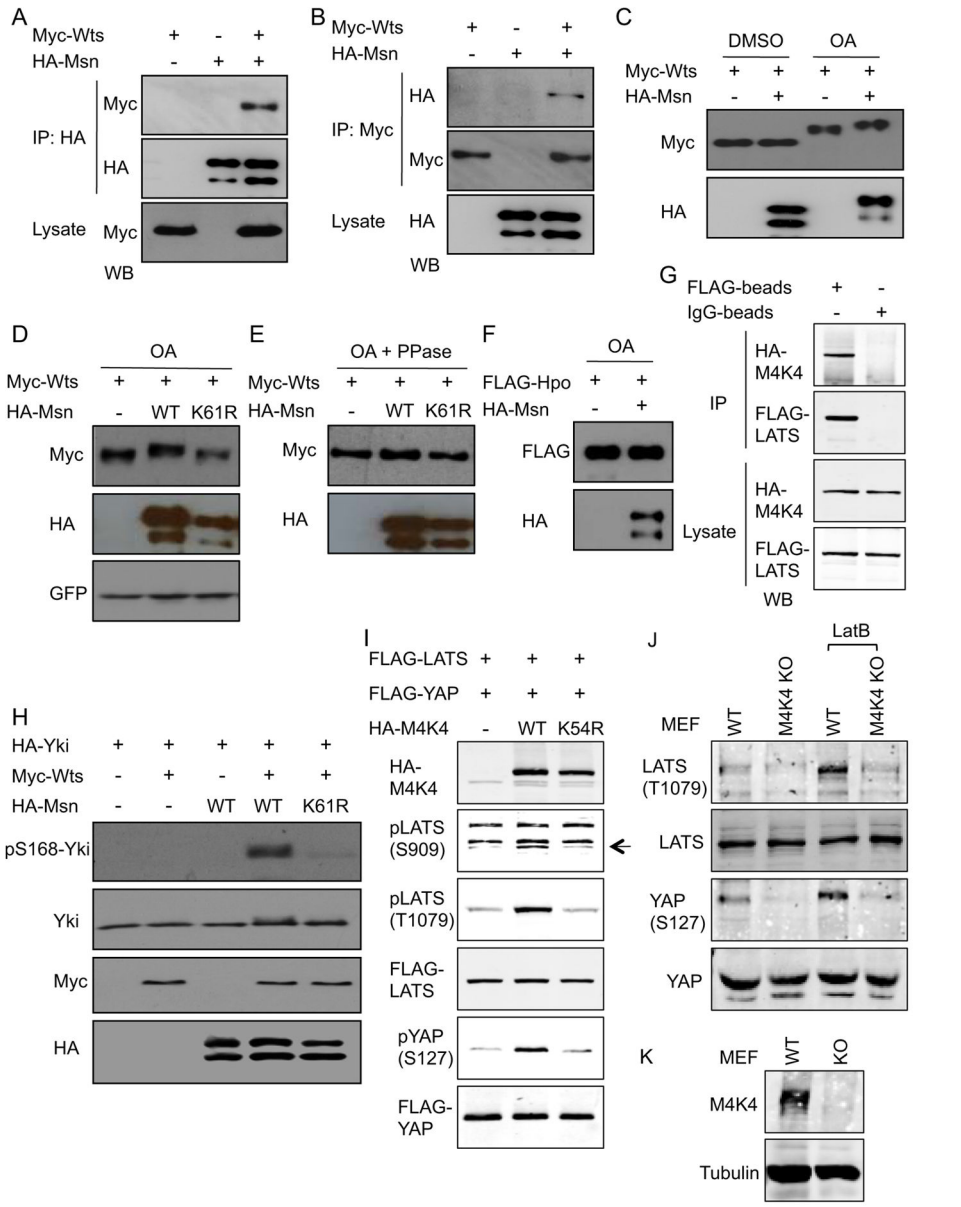

Figure 6. Physical interaction between Msn and Wts is conserved

(A, B) The indicated plasmids encoding the tagged constructs of Wts and Msn were transfected into S2 cells. The extracts were used for IP and Western blots (WB) using the indicated antibodies. (C–F) The indicated tagged protein constructs were transfected into S2 cells. 48 hours after transfection, the cells were treated with okadaic acid (OA) or the DMSO solvent control for 4 hours and then used immediately for extract preparation and subsequently for WB. The GFP in panel D was expressed from a co-transfected plasmid. The phosphatase treatment (PPase) was carried out by adding the enzyme to the extracts and incubated for 30 minutes immediately followed by SDS gel separation. (G) The plasmids encoding HA-MAP4K4 or FLAG-LATS2 were co-transfected into HEK293 cells and the extracts used for IP using anti-FLAG or control beads. The binding proteins were then subject to SDS gel separation and WB using the HA or FLAG antibodies. (H) Co-

transfection of the plasmids as indicated into S2 cells were performed and the cell extracts were used for WB. (I) The plasmids encoding the indicated tagged proteins were co-tansfected into HEK293 cells and the extracts used for WB using antibodies against HA, FLAG, pYAP or pLATS, which detect phosphorylation at the indicated a.a. residues. (J–K) Mouse embryo fibroblasts (MEFs) were from Map4k4 loxP/UBC-cre/ERT2 mice. The knockout (KO) MEFs were treated with tamoxifen to induce the Cre-mediated recombination and the untreated cells were used as wild type (WT). Extracts of these cells were used for Western blot using the antibodies as indicated.

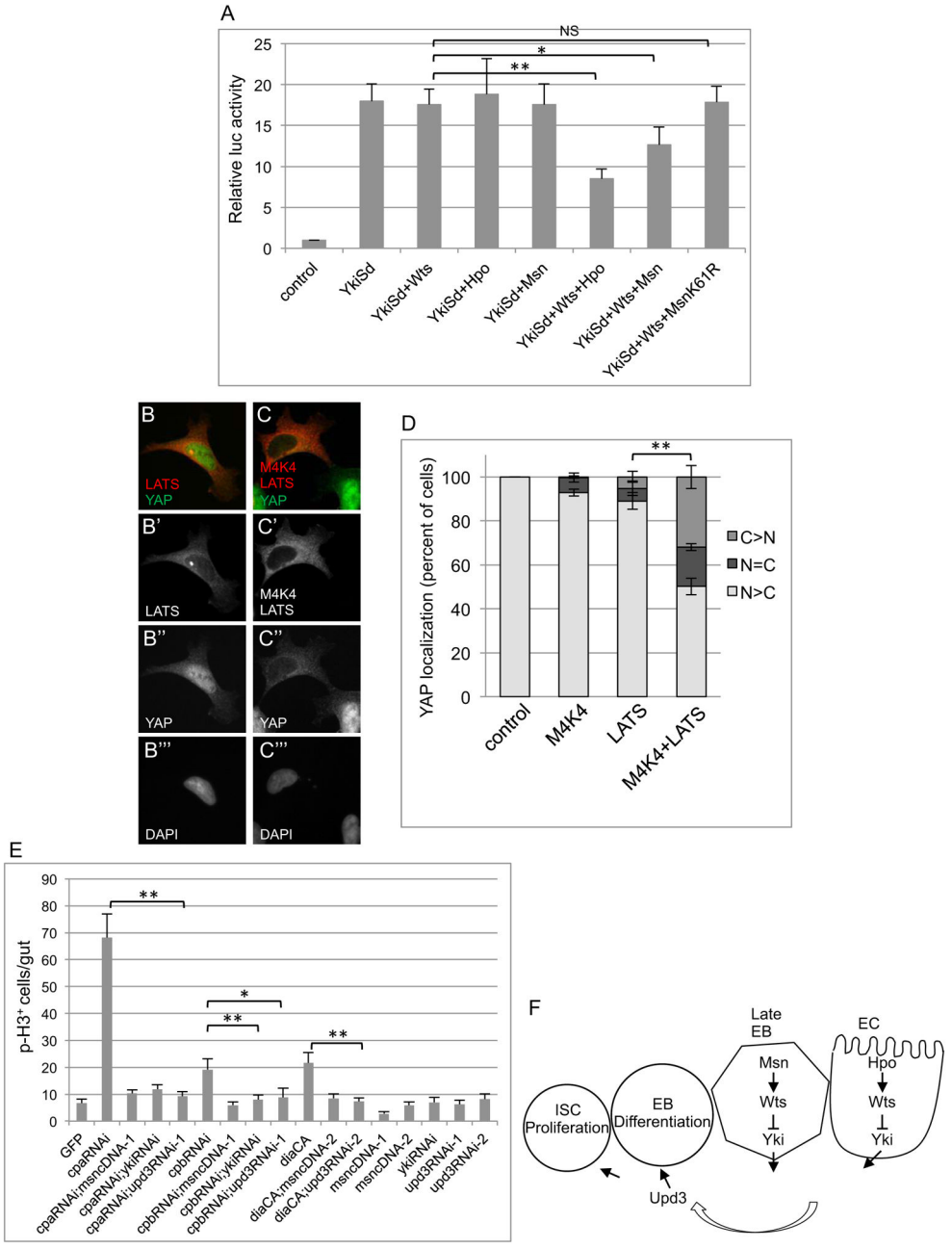

Figure 7. Functional interaction of Msn and Wts leads to Yki inactivation

(A) The *3xSd2-Luc* reporter and other plasmids encoding the indicated proteins were co-transfected into S2 cells. The luciferase assay was performed using the extracts from cells 48 hours after transfection. * is $p<0.05$. (B–D) Nuclear/cytoplasmic localization of endogenous YAP was visualized by immunofluorescent staining. HA-MAP4K4 and low levels of FLAG-LATS2 were transfected in 293A cells plated at low density such that most control cells have nuclear YAP. Panels B and C are representative examples of the signal for the stained proteins as indicated. YAP localization was examined under the microscope and scored into three different categories: mostly cytoplasmic (C>N), equally distributed (N=C)

or mostly nuclear (N>C). The bar graph represents the average and standard deviation of three independent experiments (n>100) expressed as percent of cells counted. (E) The transgenic RNAi constructs of Capping Protein A (cpa), B (cpb) and expression construct of constitutively active Diaphanous (Dia^{CA}) were crossed with the $Su(H)Gal4^{ts}$ flies. Flies with *msn* cDNA, *upd3* RNAi and *yki* RNAi constructs were also crossed together as indicated. Midguts were dissected after placing the flies for 5 days at 29°C, and p-H3 staining and counting were performed. (F) A model illustrating the function of Msn in adult midgut homeostasis. Msn forms a complex with and modifies Wts, which leads to increased phosphorylation and negative regulation of Yki. The Yki-regulated expression of the JAK-STAT ligand Upd3 is an essential effector of this pathway from the EBs. Early EBs frequently do not show the *upd3-lacZ* expression even after *msn* RNAi (Fig. 3D–D″, arrowheads), while intermediate sized cells in msn^{RNAi} and *msn* mutant MARCM clones express *upd3-lacZ* (see Fig. 3D and 3F). Therefore, the initial cause of over-proliferation phenotype after loss of Msn should be mainly from the late EBs.